



## **Supplemental Material to:**

**Péter Nagy, Manuéla Kárpáti, Ágnes Varga, Karolina Pircs,  
Zsolt Venkei, Szabolcs Takáts, Kata Varga, Balázs Érdi,  
Krisztina Hegedűs, and Gábor Juhász**

**Atg17/FIP200 localizes to perilyosomal Ref(2)P  
aggregates and promotes autophagy by activation of  
*Atg1* in *Drosophila***

**Autophagy 2014; 10(3)**

**<http://dx.doi.org/10.4161/auto.27442>**

**[www.landesbioscience.com/journals/autophagy/article/27442](http://www.landesbioscience.com/journals/autophagy/article/27442)**

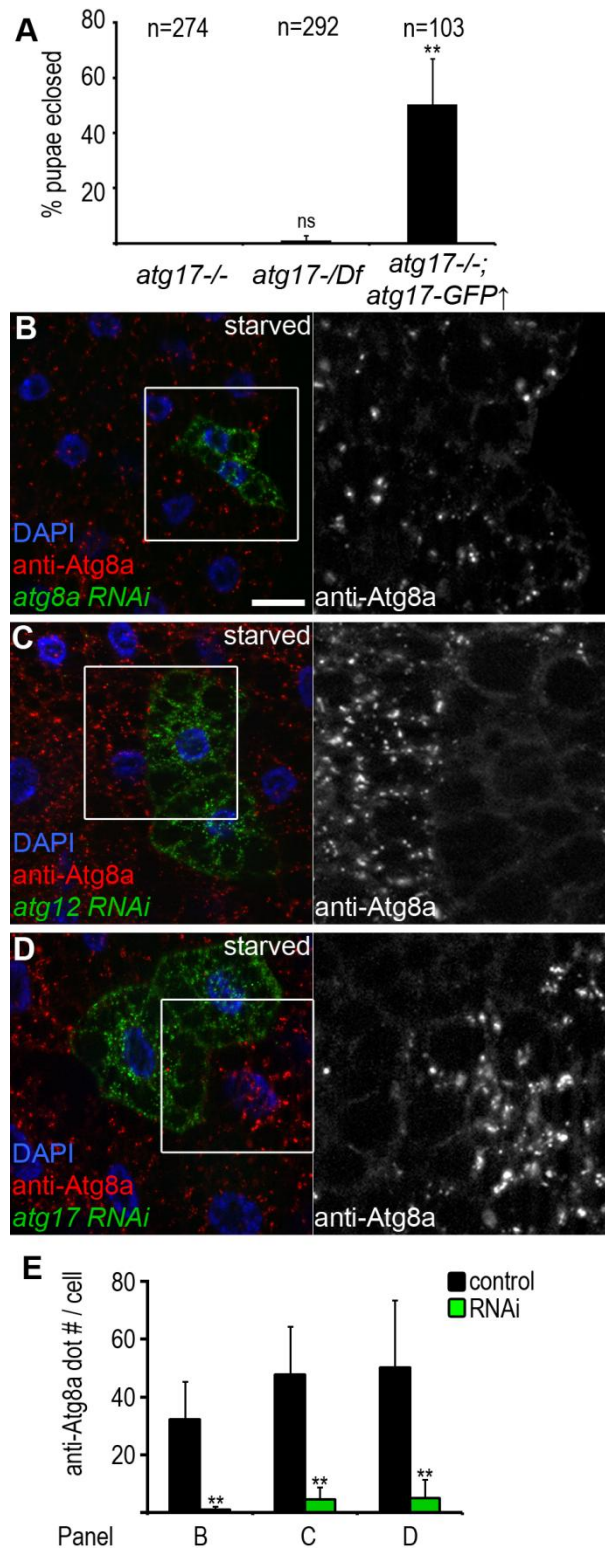


**Figure S1.** *atg17* mutant lethality and anti-Atg8a data. (A) Homozygous *atg17*[*d130*] null mutants exhibit fully penetrant pharate adult lethality: adults are completely formed but do not manage to leave the pupal case. Adult escapers are found rarely in transheterozygotes (*atg17*[*d130*] in trans with *Df*(3*R*)*BSC464*, a large deficiency including this locus): only 3 out of 292 flies eclosed. Low-level expression of *UAS-atg17-GFP* mediated by an uninduced *hs-*

*Gal4* driver rescues the lethality of *atg17* null mutant homozygotes. **(B to D)** Immunostaining experiments using our novel anti-Atg8a antibody reveal that endogenous Atg8a-positive autophagosome formation is strongly impaired in Lamp1-GFP marked *atg8a* **(B)**, *atg12* **(C)** and *atg17* **(D)** RNAi cells compared to neighboring control cells. **(E)** Quantification of data from B-D; n=10/genotype. Scale bar equals 20  $\mu$ m for B to D. Error bars: s.d., ns, not significant, \*\* P<0.01.

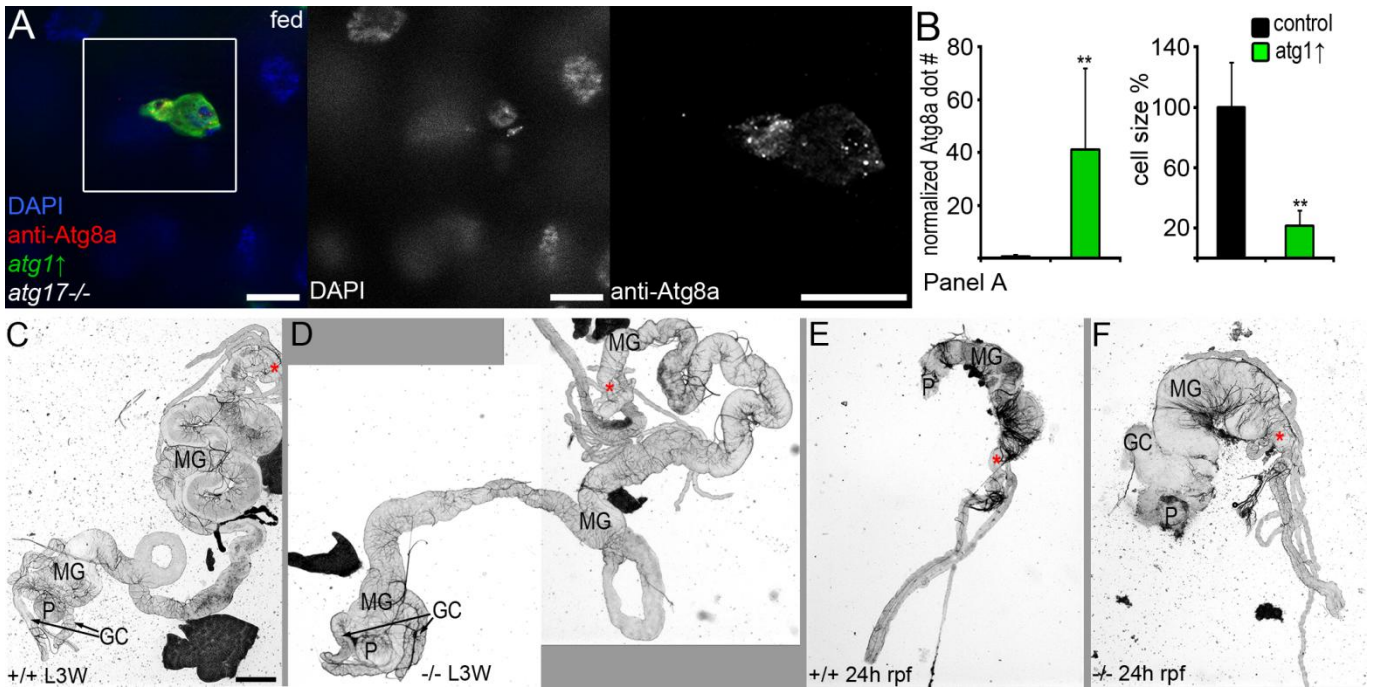


**Figure S2.** Atg1 overexpression and developmentally programmed shrinkage of the polyploid midgut during metamorphosis in *atg17* null mutants. (A) Overexpression of Atg1 in GFP-expressing fat body cells induces Atg8a-positive autophagosome formation and reduces cell size in *atg17* null mutants. The DAPI channel is shown separately to illustrate the size of the nuclei, and the anti-Atg8a channel is shown enlarged from the boxed area. (B) Quantification of data from A; n=10. (C to F) L3 stage wandering larval midguts (MG, located between the proventriculus, P, and the branching out of Malpighian tubules, \*) appear similar in controls (C) and *atg17* null mutants (D). Involution of gastric caeca (GC) and shrinkage of larval midguts is defective in *atg17* null mutants at 24 h relative to puparium formation (rpf), which is obvious based on the much bigger size of the midgut (F) compared to similarly aged controls (E); n=10/genotype. Scale bar in B equals 20  $\mu$ m, and 160  $\mu$ m for C to F.

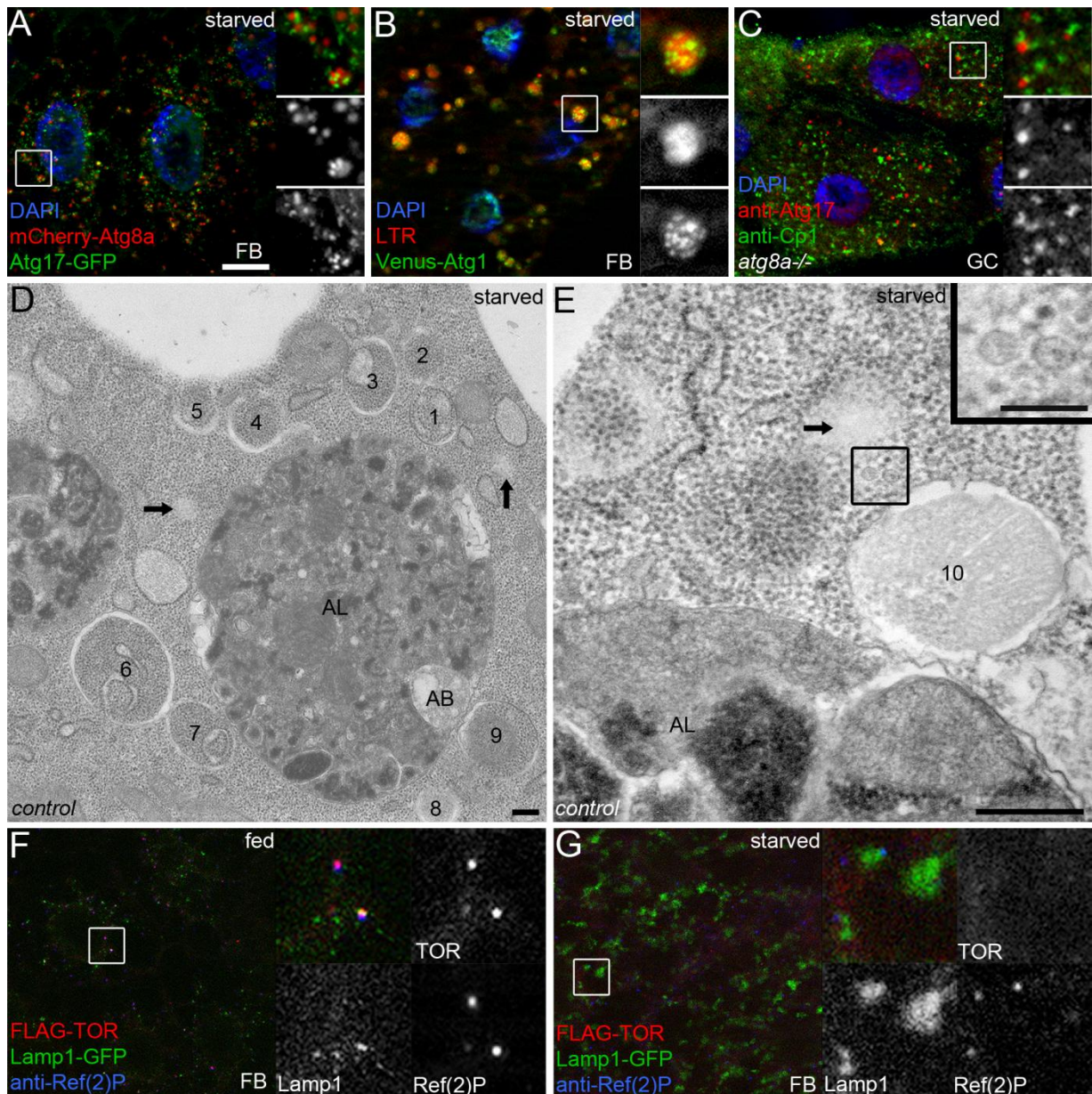


**Figure S3.** Preautophagosomal structures assemble near lysosomes. **(A)** Atg17-GFP dots are tightly associated with large mCherry-Atg8a-positive autolysosomes (large red structures). **(B)** Venus-Atg1 puncta cluster around LTR-positive autolysosomes. **(C)** Endogenous Atg17 localizes near Cp1-positive lysosomes in starved *Atg8a* null mutant gastric caeca. **(D, E)** Transmission electron micrographs of fat body cells from starved control larvae reveal ribosome- and organelle-free regions that may correspond to protein aggregates (arrows) near autolysosomes (AL) in panels **(D)** and **(E)**. Note the typical cluster of autophagosomes (marked by numbers) that surround the autolysosome in **(D)**. AB indicates an autophagic body inside the autolysosome, with its undigested cargo still surrounded by a membrane, which was originally the inner membrane of an autophagosome before fusion. 40-

to 60-nm vesicles are seen between a ribosome-free cytoplasmic region and an autophagosome in the vicinity of an autolysosome, and are shown enlarged in the inset of panel **(E)**. **(F,G)** Punctate FLAG-TOR colocalizes with Ref(2)P in fat bodies of well-fed larvae **(F)**. Starvation results in dispersion of FLAG-TOR but not Ref(2)P, which remains associated with Lamp1-GFP marked lysosomes **(G)**. Scale bar equals 20  $\mu\text{m}$  for panels A-C,F,G. Scale bars equal 300 nm in D, E and 100 nm for the inset in E. FB, fat body; GC, gastric caeca.

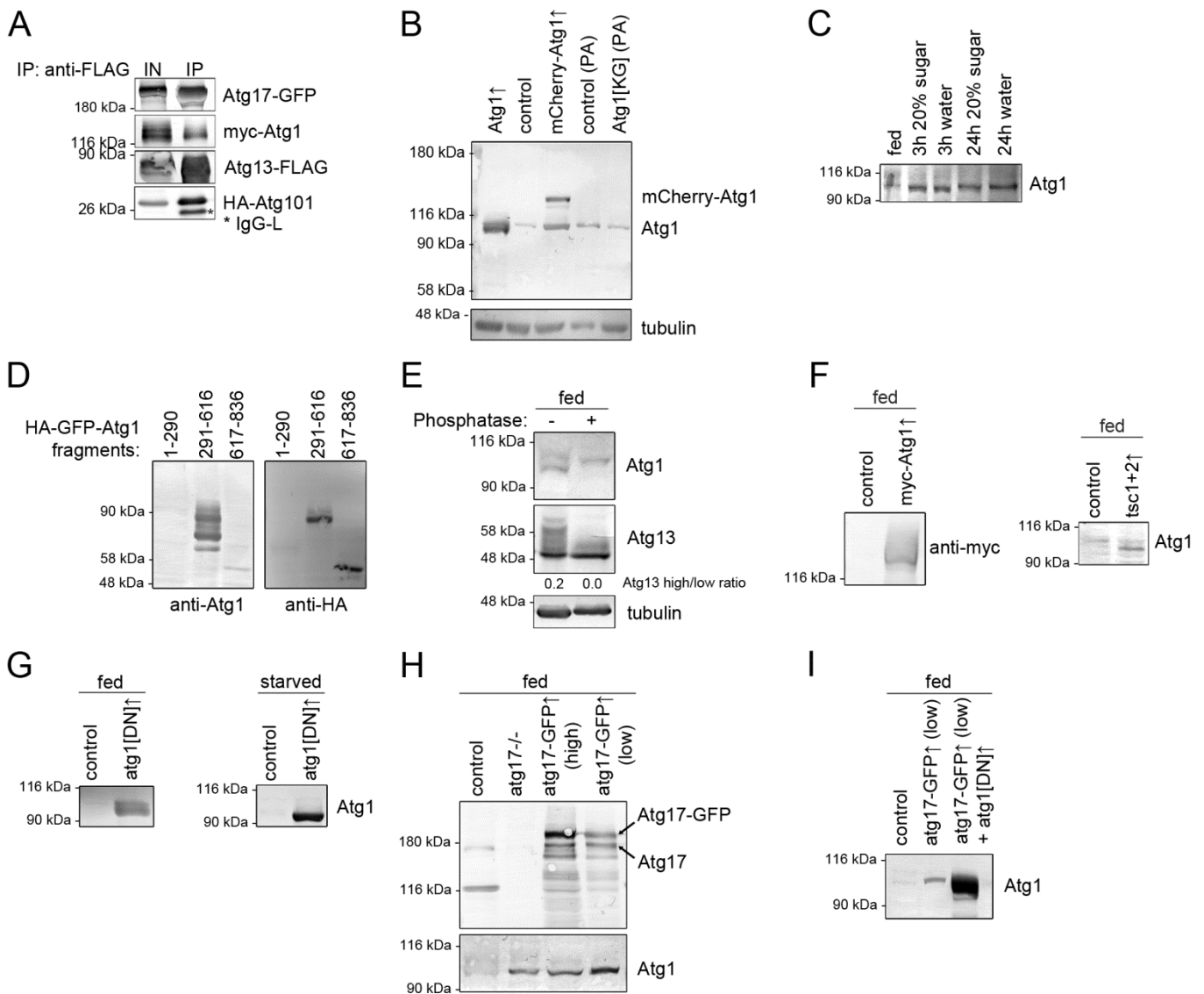


**Figure S4.** Additional data on the Atg1 complex. **(A)** Atg17-GFP, myc-Atg1 and HA-Atg101 immunoprecipitate with Atg13-FLAG in larval lysates. **(B)** Western blots using our polyclonal anti-Atg1 antibody detect endogenous and overexpressed wild-type or mCherry-tagged Atg1 in larval extracts. Reduced amounts of Atg1 are seen in *atg1* hypomorph mutant pharate adults (PA) compared to controls. **(C)** Atg1 is barely detected in fat body extracts of well-fed animals, but appears as a major band upon starvation. **(D)** Our anti-Atg1 antibody recognizes the middle region of Atg1, based on western blots of HA-GFP-tagged Atg1 fragments. **(E)** Phosphatase treatment of fat body samples from well-fed larvae reduces endogenous Atg1 and Atg13 practically to single bands. **(F)** Expression of myc-Atg1 and endogenous Atg1, see also western blots in Fig. 7D. **(G)** Expression of Atg1, see also western blots in Fig. 7E. **(H)** Anti-Atg17 and Atg1 western blots, see also Fig. 7F. Note that constitutive expression (high) of Atg17-GFP results in higher protein levels than transient

expression (low) in fat body extracts of well-fed animals. **(I)** Endogenous Atg1 western blot, see also Fig. 7G.

1 METDLNSQDRKDLDFKFKFFALKTVQVIVQARLGEKICTRSS.SSPTGSDWFN...LAIK HsAtg13  
 1 HSAQRLENAAEERDLKFKFKFLV LKSTQVVVQSRLEKMQTCN..PLAGSDWFN...IAVQ DmAtg13  
 1 MVNEYDTYNKWLKFFSVRMVQSI IQSRLCDETESKCVPYSEN AVDFWN...MRID CeAtg13  
 1 MVAEEDIKQVQLQLDSF LKTTLLICSTESSRYQSSTEN..IFLFDTTWEDHSELVS ScAtg13

HORMA domain in  
 ScAtg13 (1 to 268)  
 (1 to 205 in DmAtg13)

57 DIPEVT...HEAKKAL...ACQLPAVGRSMCVEISLKTSEGD.....SME HsAtg13  
 56 DEPEVL...DETKRALNLKTGESILQRLPLCVEISLKTTEGD.....QMV DmAtg13  
 53 ELGEIS...AYLKSNI...KSYPPVGTLTLEFLLYTPSCQ.....LLP CeAtg13  
 58 ELPEIISKWSHYDGRKELPPLVVEYLDLRQLNSSHVRLKDEHGLWNVCKGTTKQEIY ScAtg13

Atg1 and Atg17  
 binding region in  
 ScAtg13 (350 to 550)

96 LEIWCLEMNEKCD.....KEIKVSYTVYNRISLLKSLAITRVTPAYRLS. HsAtg13  
 98 LEVWSLDLQPPQNGSPATNDLNPEGQTLKAAHATYNRMGIMKSLISLRTTPAYKLS. DmAtg13  
 90 LEAWILSSSEG.....TDCSRNELYHDMSTLLRSATVSAVMPMERLYV CeAtg13  
 118 MERWLTLELDNSSP.....TFKSYSEDETVDNELSKQLVLLFRYLTLIQLLPTTELYQ ScAtg13

ULK1, ULK2 and  
 RB1CC1 binding  
 region in HsAtg13  
 (384 to 517), which  
 corresponds to  
 amino acids 398 to  
 523 in DmAtg13

142 .....RKQG.HEVYLIRIYFGEVQL HsAtg13  
 157 .....RRCQPDYSYGFYRIYVDRPQV DmAtg13  
 135 .....KKQHLETFVIMYRVFENDISS CeAtg13  
 171 LLIKSYNGPQNEGSSNPITSTGPLVSI RCTCVLDGSKPILSKGRIGLSKPIINTVSMALNE ScAtg13

162 SCLGECFQTVRVGTVPVCTITLSCAYRINLAFMSRQFERTPPIMGIIIDHFVDRPYP HsAtg13  
 178 HTLGECHKHVKIGQLSTIVCSLVM SVAYRTKLTISP TAAQSESNTIM.LKSDHFRFATDA DmAtg13  
 156 .DMCKKTRKIGELVSKFCNISLDLHYRTSMHFEEPE.....EIAVTPV CeAtg13  
 231 SNLPAHL DQKXITPVWTKFQLLRYSVSTRDWKFEINNTNDELFSARHASVSHNSQGPQN ScAtg13

222 SSSPMHPCNY.....RTAGEDTGVIIYPSVEDS QEVCTTSSTSPSPQLSSSRL HsAtg13  
 237 NTPGNQQTQ.....NGTVVAKKLGALNPAQGTADRRFDIEKP.LRPGAF DmAtg13  
 200 EDVVEEIDDG.....EKTVDENIQTRIVSECVPIADAKRRK.....ASGSV CeAtg13  
 291 QPEQEGQSDQDIGKRQPQFQQQQQFQQQQQQRQHQQVQTQQRQIPDRSLSLSPC ScAtg13

270 SYQPALGVGSADLAVPVVFAAGLNATHPHQLMVPKEGGVP.....LA HsAtg13  
 284 TDMGKLGKQYTEDDFVLPETPFEFWLLRCRGSVESLNRLDNNS.....VA DmAtg13  
 242 ESATSAGSSTREAAAPRFILGQSTSSSEDSRHS DVQNSYEEDH.....KP CeAtg13  
 351 TRANSFEPQSWQKKVYPIISRQVQPFKVGSI GSGSASRNPSNS SFFNQPPVHRPMSSSNYC ScAtg13

314 PNQPVHCTQADQERLATCTPS...DRTHCAATPSSSEDTETVSNSS EGRASPHDVL ETIF HsAtg13  
 328 SVMISNNNNSTQDSKFNQISN...LNNSAGFKSFEKNSENSVSPIKSLLTASATATYR DmAtg13  
 286 SLADLRNHSFPFVNLLQSAVN...PANGTKKNSSTCLNSPKSTPEKPTIEKVAESFR CeAtg13  
 411 PQMNIECTSVGSTSKYSSSEGNIRRHSSVKTENA EKVS KAVKSPLQPQESQEDLMDLVK ScAtg13

371 VRKVGVA.....FVNKPINQVTLTSLDIFAMFAPKNLE... HsAtg13  
 385 HHS EFS.....LQPPDDNLLKLELHFFASPTS HVND... DmAtg13  
 343 AA WIDE.....VVFEEDED...EELPLDSMELSEDS... CeAtg13  
 471 LLEKPDLTIKKTSGNPPNINISDLIRYQNLKPSNDLSEDL SVSLSMDPNHTYHRGR ScAtg13

404 .....LEDTFMVNPPDSPETESP LQGS LHSDCSSGCSGNT HDDFVMIDFKPAFSKDD HsAtg13  
 418 .....LAKFYRECYHAPPLKGLNELQAEISSISSTPPASSSGG...VAACGPTAAATA DmAtg13  
 371 .....FVHFNQLSDFCGAPSLGNELGDY LKQLKTAPDMTEG..... CeAtg13  
 531 SDSHSP LPSISFSMHYGSLN SRMSQGANASHL LARGGNSSTALNSRRNSLDKSNKQC ScAtg13

458 IL.....PMDLGTFRYEFQNPQLSSLSIDIGAQSMAEDLDSPEKLA VHEKNVREF HsAtg13  
 469 IA.....TSSADASAMDDL SRQLLEQFETSLEDYDKLV SQFLTGSSSTGSRSSGGI DmAtg13  
 408 .....DIDICNMDLKTLEKISSQTAFNFNFLKHV CeAtg13  
 591 MSGLPPIFGGESTSYHHDNKIQKYNQLGV EEDDENDRLLNQMGNSATKFKSISIPRSI ScAtg13

⊠ non conserved  
 X similar  
 X conserved  
 X all match

510 DARVETLQ HsAtg13  
 520 QMSN DmAtg13  
 438 NFSFDE CeAtg13  
 651 DSISSEFIKSRIPIRQPYHYSQPTTAPFQAQAKFHKPA NKLI DNGNRSNSNNNNHNGNDA ScAtg13

711 VGVMHNDEDDQDDDLVFFMSDMNLSKEG ScAtg13

**Figure S5.** Multiple sequence alignment of human (Hs), fly (Dm), worm (Ce) and yeast (Sc) Atg13 proteins. The HORMA (Hop1p, Rev1p and Mad2) domain appears conserved, while only limited similarity is detected in the middle and C-terminal regions.